# Recent Progress in the Development of Mid-Infrared Medium Resolution Spectrometer (MRS) installed in SPICA/MCS

Itsuki Sakon*[a], Hirokazu Kataza[b], Takashi Onaka[a], Ryou Ohsawa[a], Yoko Okada[c], Yuji Ikeda[d, e], Naofumi Fujishiro[d,e], Kenji Mitsui[f], Norio Okada[f]

[a]Department of Astronomy, Graduate Schools of Science, University of Tokyo,
7-3-1 Hongo, Bunkyo-ku, Tokyo 113-0033, Japan
[b]Institute of Space and Astronautical Science, Japan Aerospace Exploration Agency,
3-1-1 Yoshinodai, Chuo-ku, Sagamihara, Kanagawa 252-5210, Japan
[c]Universität zu Köln, I. Physikalisches Institut,
Zülpicher Str. 77, 50937 Köln, Germany
[d]Photocoding, Inc., 61 Ikeda-cho, Iwakura, Sakyo-ku, Kyoto 606-0004, Japan
[e]Deprtment of Physics, Faculty of Science, Kyoto-Sangyo University,
Motoyama,Kamigamo, Kita-Ku, Kyoto-City 603-8555, Japan
[f]Advanced Technology Center, National Astronomical Observatory of Japan,
National Institutes of Natural Sciences, 2-21-1 Osawa, Mitaka,Tokyo 181-8588, Japan

## ABSTRACT

Mid-infrared Medium Resolution Spectrometer (MRS) is one of the key spectroscopic modules of Mid-Infrared Camera and Spectrometers (MCS) that will be onboard SPICA. MRS is an Echelle Grating spectrometer designed to observe a number of fine structure lines of ions and atoms, molecular lines, and band features stemming from solid particles and dust grains of the interstellar and circumstellar medium in the mid-infrared wavelength range. MRS consists of two channels; the shorter wavelength channel (MRS-S) covers the spectral range from 12.2 to 23.0 micron with a spectral resolution power of R~1900—3000 and the longer wavelength channel (MRS-L) covers from 23.0 to 37.5 micron with R~1100—1500 on the basis of the latest results of the optical design. The distinctive functions of the MRS are (1) a dichroic beam splitter equipped in the fore-optics, by which the same field of view is shared between the two channels, and (2) the small format image slicer as the integral field unit installed in each channel. These functions enable us to collect continuous 12—38 micron spectra of both the point-like and diffuse sources reliably with a single exposure pointed observation. In this paper, the specifications and the expected performance of the MRS are summarized on the basis of the latest results of the optical design. The latest progress in the development of the key technological elements, such as the Dichroic Beam Splitter and the Small Format Monolithic Slice Mirrors, are also reported.

**Keywords:** infrared astronomy, infrared instrumentation, SPICA

## 1. INTRODUCTION

SPICA (Space Infrared Telescope for Cosmology and Astrophysics) is a next generation Infrared Space Mission with a cryogenically cooled ~3.2m telescope (Nakagawa et al. 2012) and the core spectral range of SPICA resides between 20 and 200μm, most of which will not be covered by the JWST efficiently. In this spectral range, there exist a number of fine structure lines of ions and atoms, molecular lines, and band features stemming from solid particles together with the dust continuum emission. Moreover,

many important optical and near-infrared line and band features of high red-shift objects also come into this spectral range. Whereas SAFARI (Roelfsema et al. 2012) provides us spectral mapping capability with a spectral resolution power of R~3000 in the far-infrared wavelength, mid-infrared spectral mapping capability with adequate spectral resolution power to detect those spectral features is strongly required for the Mid-Infrared Camera and Spectrometer (MCS; Kataza et al. 2012). Mid-Infrared Medium Resolution Spectrometer (MRS) is one of the spectroscopic modules of the MCS that will be onboard SPICA and is designed to meet with such request. MRS will provide significant and crucial information on the evolution of various phases of the interstellar medium (ISM) and will play a key role in the studies on interstellar and circumstellar physics and chemistry. The description on the specification and the expected performance of MRS is given in Section 2 and the latest development status of key technical issues, particularly on the Dichroic Beam Splitter and small-format image slicer, is reported in Section 3.

*isakon@astron.s.u-tokyo.ac.jp; phone +81 3 5841-4276; fax +81 3 5841-7644

## 2. MID-INFRARED MEDIUM RESOLUTION SPECTROMETER (MRS)

### 2.1 The Optical Design and Specifications of MRS

Mid-infrared medium resolution spectrometer (MRS) installed in the SPICA Mid-Infrared Camera and Spectrometer (MCS; Kataza et al. 2012) is an Echelle Grating spectrometer designed to observe a number of fine structure lines of ions and atoms, molecular lines, and band features stemming from solid particles and dust grains of the interstellar and circumstellar medium in the mid-infrared wavelength range. MRS consists of two channels; MRS-S covers the spectral range from 12.2μm to 23.0μm with a spectral resolution power of R~1900–3000 and MRS-L covers from 23.0μm to 37.5μm with R~1100–1500. The same field-of-view (FOV) is shared between the two channels by means of the beam splitter. The optical layouts of SPICA/MCS/MRS-S and MRS-L based on the latest results of the optical design are shown in Figure 1.

Each channel equips the small format image slicer as the integral field unit preceding the spectrograph optics. In the case of MRS-S, the "reflected" beam by the beam splitter is converted into the F/10 beam by means of the two free-form mirrors and is refocused on the slice mirror. The field-of-view with a size of 6 arcsec by 12 arcsec on the refocused plane is divided into 5 slitlets, each of which has a size of 1.2 arcsec width and 12 arcsec length, by the slice mirror. Then, their pupil images are produced on the spherical pupil mirrors, which are placed independently on the output pupil positions. Finally, the slit images refocused by the 5 spherical pupil mirrors are aligned on the pseudo slit mirrors, forming in a pseudo slit image. In the case of MRS-L, in a similar way, the "transmitted" beam by the beam splitter is converted into the F/10 beam by means of the two free-form mirrors and is refocused on the slice mirror. The field-of-view with a size of 7.5 arcsec by 12 arcsec on the refocused plane is divided into 3 slitlets, each of which has a size of 2.5 arcsec width and 12 arcsec length, by the slice mirror. Then their pupil images are produced on the spherical pupil mirrors, which are placed independently on the output pupil positions. Finally, the slit images refocused by the 3 spherical pupil mirrors are aligned on the pseudo slit mirrors, forming in a pseudo slit image. The lengths of the pseudo slits of MRS-S and MRS-L lengths are 60 arcsec and 36 arcsec, respectively.

As for the MRS-S, the output F/10 beam from the pseudo slit is cross dispersed so that the spectrum over 4 different orders from $m=5th$ to $8th$ falls on the Si:As 2K2K detector array. The shortest wavelength of the highest Echelle order $m=8th$ is set to 12.2μm and the longest wavelength of the lowest Echelle order $m=5th$ is set to 23.04μm. Within this spectral range, the blaze function achieves the efficiency of >40% at any wavelength. As for the MRS-L, the output F/10 beam from the pseudo slit is cross dispersed so that the spectrum over 6 different orders from $m=10th$ to $15th$ falls on the Si:Sb 1K1K detector array. The shortest wavelength of the highest Echelle order $m=15th$ is set to 23.00μm and the longest wavelength of

the lowest Echelle order $m=10th$ is set to 37.53μm. Within this spectral range, the blaze function achieves the efficiency of >40% at any wavelength.

The wavelength range covered by the $m^{th}$ order spectra is summarized in Table 1. $\lambda_{min}^m$ and $\lambda_{max}^m$ are defined by the wavelengths where the blaze function of the Echelle grating drops to the efficiency of 40% in the $m^{th}$ order and $\lambda_b^m$ is the blaze wavelength in the $m^{th}$ order. We note that the redundant spectral parts of the $m^{th}$ order spectrum are defined as the 20% of the whole spectral range of the $(m+1)^{th}$ order $(\lambda_{max}^{m+1}$-$\lambda_{min}^{m+1})$ so that the spectra shared by adjacent orders can be combined to achieve better sensitivity. In this sense, the spectrum in the wavelength range from 22.64μm to 23.62μm is redundantly obtained both by MRS-S and MRS-L on the detector arrays if including the redundant spectral parts mentioned above. The spectral resolution powers of MRS-S and MRS-L for a point source are shown in Figure 2 as a function of wavelength.
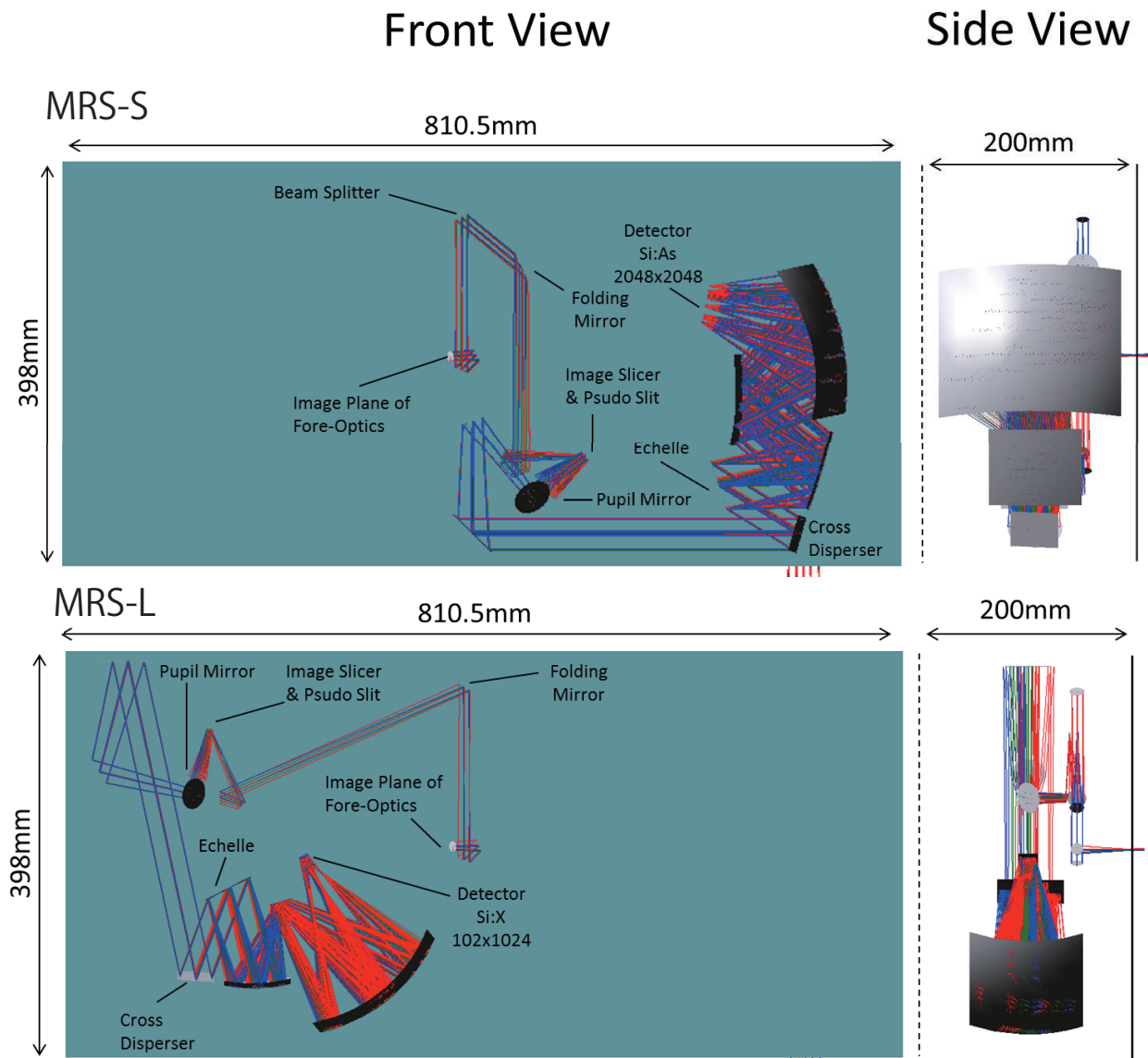


Figure 1. The optical layouts of the MRS-S (top) and MRS-L (bottom) channels of SPICA/MCS/MRS

Table 1. Spectral Format of MRS-S and MRS-L on the detector arrays

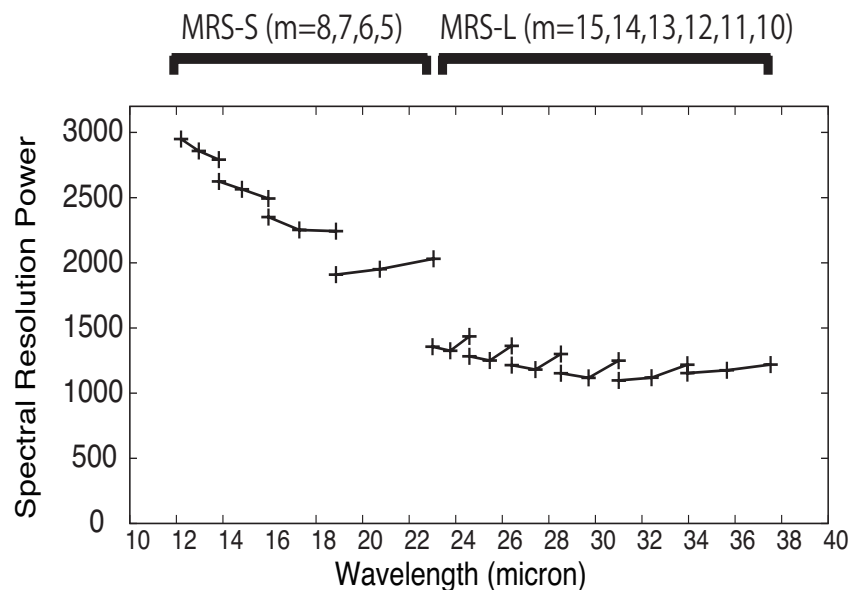| MRS-S | | | | MRS-L | | | |
|---|---|---|---|---|---|---|---|
| Echelle Order | $\lambda_{min}^m$ (μm) | $\lambda_b^m$ (μm) | $\lambda_{max}^m$ (μm) | Echelle Order | $\lambda_{min}^m$ (μm) | $\lambda_b^m$ (μm) | $\lambda_{max}^m$ (μm) |
| m=5 | 18.85 | 20.74 | 23.04 | m=10 | 33.95 | 35.65 | 37.53 |
| m=6 | 15.95 | 17.28 | 18.85 | m=11 | 31.00 | 32.41 | 33.95 |
| m=7 | 13.83 | 14.81 | 15.95 | m=12 | 28.52 | 29.71 | 31.00 |
| m=8 | 12.20 | 12.96 | 13.83 | m=13 | 26.41 | 27.42 | 28.52 |
| -- | -- | -- | -- | m=14 | 24.59 | 25.46 | 26.41 |
| -- | -- | -- | -- | m=15 | 23.00 | 23.77 | 24.59 |



Figure 2. Spectral resolution powers of MRS-S and MRS-L for a point source

## 2.2 Expected Performance of MRS

The sensitivity and the saturation limit of MRS are estimated by assuming appropriate telescope parameters and detector performances taking account of their latest development status (e.g., Matsuhara, et al., 2012; Wada et al. 2012; Kataza et al. 2012). The longest ramp duration is defined so that the mean number of pixels affected by cosmic ray hit events during an exposure should not exceed 4% of the whole pixels of a detector array. Assuming that the cosmic ray hit event rate at L2 point is $5×10^4$ m$^{-2}$ sec$^{-1}$ (Swinyard et al. 2004) and that 4 pixels are affected by a single event, the longest ramp duration time for MRS-S, which adopts the Si:As detector array with a pixel scale of 25 μm pix$^{-1}$, is set to 300 sec and that for MRS-L, which adopts the Si:Sb detector array with a pixel scale of 18 μm pix$^{-1}$, is set to 600 sec. The shortest ramp duration is set to 2sec for both channels. In our calculations, the high background case assumes the condition of the ecliptic plane at β= 0.0deg and ε=60deg, while the low background case assumes that of the ecliptic pole at β= 90deg. Assuming that the background emission is dominated by the zodiacal emission, the background emission in the high background case is modeled

with blackbody of T=268.5K normalized to 80 MJy/sr at 25μm, while that in the low background case is molded with blackbody of T=274.0K normalized to 15 MJy/sr at 25μm taking account of the results of observations with ISO and IRTS (i.e., Reach et al. 2003; Ootsubo et al. 2000). The expected values of the 5σ 3600sec continuum sensitivity and line sensitivity for a point source calculated for both the low- and high-background cases are shown in Figure 3. The saturation flux density for a point source calculated for the shortest ramp duration is shown in Figure 4.
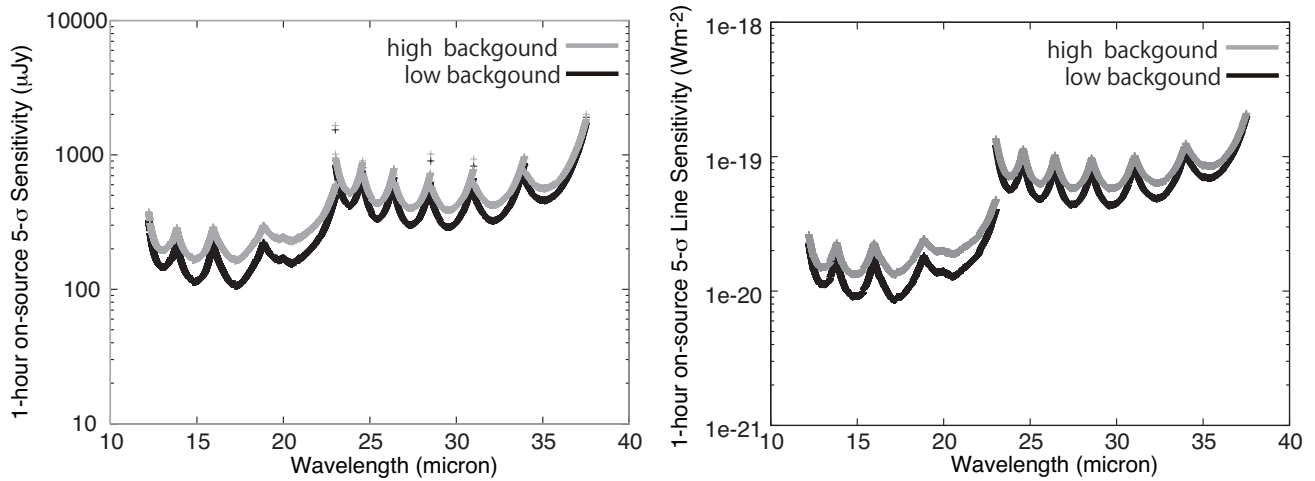


Figure 3. (a) The 3600 sec on-source 5-σ sensitivity of MRS estimated for a continuum of a point source for the cases of full spectral resolution power R (see Figure 2). (b) The 3600 sec on-source 5-σ sensitivity of MRS estimated for a line emission in units of Wm⁻². The expected sensitivities for low-background case are shown with black and those for high-background case are shown with gray.
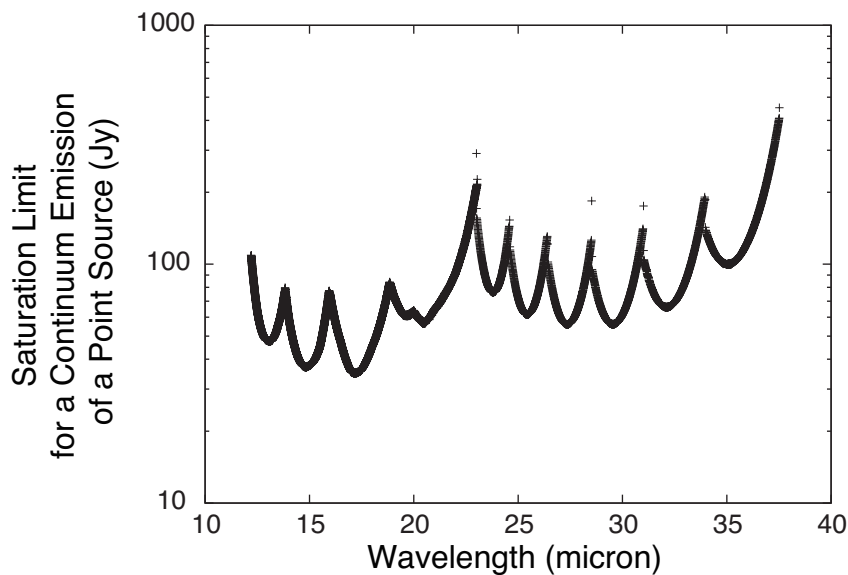


Figure 4. The saturation limit for the continuum of a point source of MRS calculated for the shortest ramp duration. The results obtained for low-background case and high-background are indistinguishable at the scale of this plot.

# 3. THE STATUS OF KEY TEHCNICAL DEVELOPMENT ISSUES

## 3.1 A Dichroic Beam Splitter (DBS) and Short Wavelength Cut Filters (SWCFs)

Based on the current optical design, the dichroic beam splitter (DBS) is placed just after the fore-optics output. The angle of incident (AOI) is set to 30deg. The nominal specification of the beam splitter is that the shorter wavelength light (12—23μm) is reflected and lead to MRS-S and that the longer wavelength light (23—38μm) is transmitted and lead to MRS-L. In order to avoid the contamination of photons by second and higher-order diffracted light, short wavelength cut filter (SWCF) is installed in each channel. Test pieces of the DBS and SWCFs are designed and produced by Infrared Filter Solution Ltd to demonstrate the technical feasibility of these elements. So far, the DBS and the SWCF for MRS-S have been procured and their cryogenic spectral characteristics have been measured.
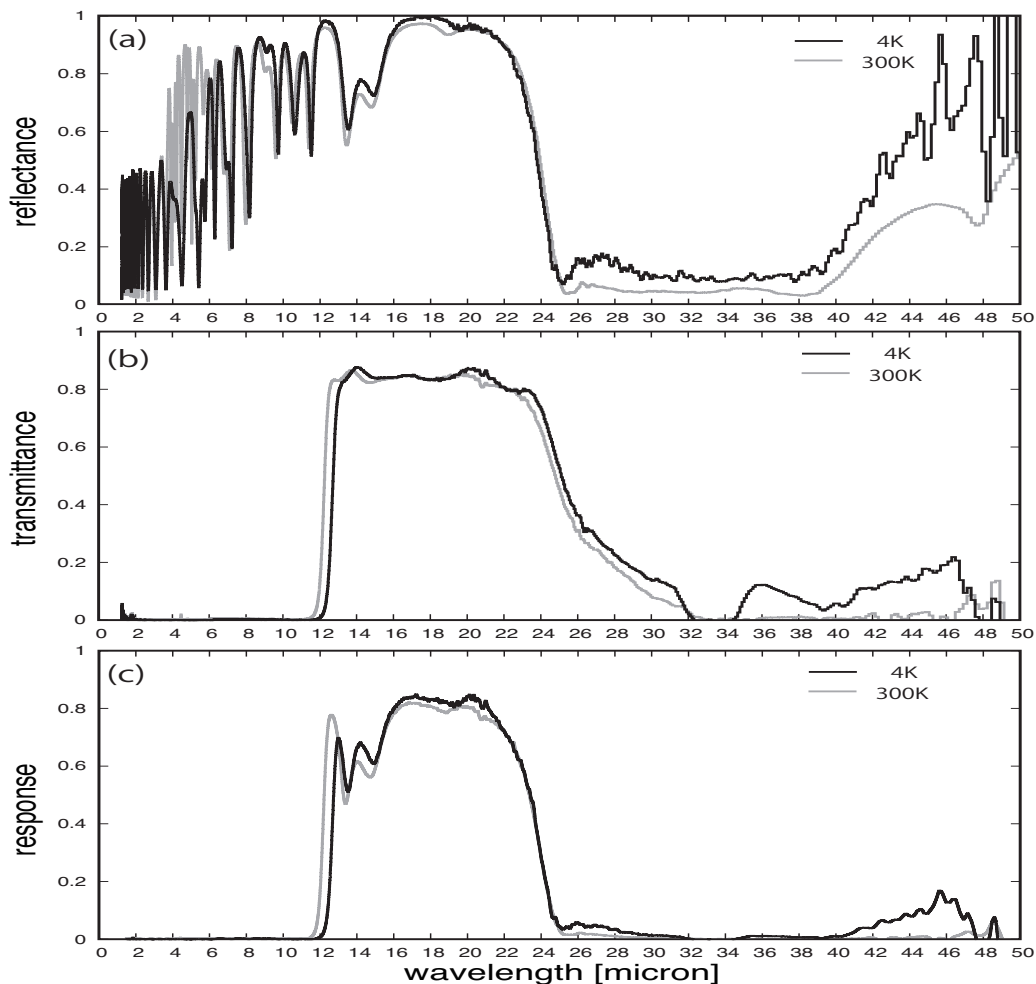


Figure 5. The spectral characteristics of the test pieces of dichroic beam splitter (DBS) and short wavelength cut filter (SWCF) used in MRS-S channel. (a) The measured reflection curves of the DBS at ambient (300K) and cryogenic (4K) temperatures are shown with gray and black, respectively. The measurement of the cryogenic reflection curve of DBS was carried out at AOI 11$^\circ$ due the constraint of our cryogenic measurement system. The measured spectrum is converted to the refection curve at default AOI 30$^\circ$ assuming the empirical wavelength shift of $\lambda_{AOI30^\circ} = 0.9888$ $\lambda_{AOI11^\circ}$ obtained from the measurements at 300K. (b) The measured transmission curves of the SWCF at AOI 0$^\circ$ used in MIRS-S channel at 300K and 4K are shown with gray and black, respectively. (c) The resultant response curves at 300K and 4K including the reflectance by DBS and transmittance by MRS-S SWCF are shown with gray and black.

The cryogenic reflection curve of DBS at AOI 30° and the cryogenic transmission curve of MRS-S SWCF at AOI 0° obtained from our measurements are shown in Figure 5 together with the results at 300K. The resultant response including the reflectance by DBS and transmittance by MRS-S SWCF achieves good blocking-capability in wavelength shorter than 12μm and good response in 12.2—23.0μm.

The measured cryogenic transmission curve of DBS at AOI 30° is shown in Figure 6 together with that at 300K. Good transmission in 24—40μm has been achieved by the latest design of the DBS test piece.
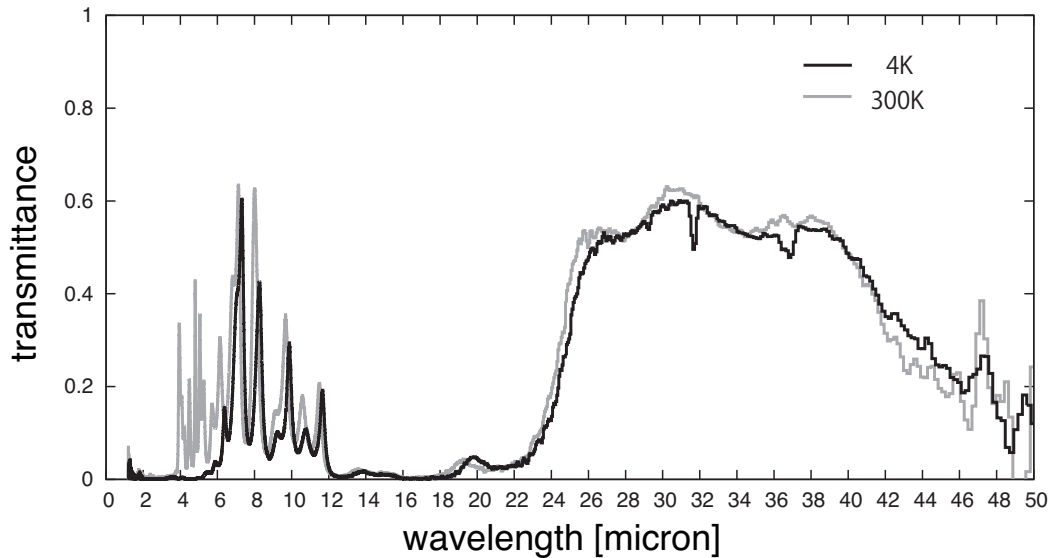


Figure 6. (a) The measured transmission curves of the DBS at ambient (300K) and cryogenic (4K) temperatures at AOI 30° are shown with gray and black, respectively.

Further optimization in the wavelength position of dichroic split for the DBS and the development of MRS-L SWCF having good response in 23.0—37.5μm and good blocking-capability in <19μm shall be required.


## 3.2 Development of Small-Format Monolithic Slice Mirror

Based on the latest optical design of the image slicer, the FOV image is refocused on the slice mirror with F/10. In the case of MRS-S, the FOV with a size of 6 arcsec by 12 arcsec is divided into 5 slitlets, each of which has a size of 1.2 arcsec width and 12 arcsec length. In the case of MRS-L, on the other hand, the FOV with a size of 12 arcsec by 7.5 arcsec is divided into 3 slitlets, each of which has a size of 2.5 arcsec width and 12 arcsec length. Based on this design, the width of the slit mirror becomes 174μm for MRS-S and 363μm for MRS-L assuming 3.0m as the size of primary mirror in diameter. The schematic design of the monolithic slice mirror for MRS-S is shown in Figure 7 (left).

A test piece of the monolithic slice mirror for MRS-S was produced experimentally by the ultra-precision cutting machine, ULG-300, with single crystal diamond bits at the Advanced Technology Center (ATC) of National Astronomical Observatory of Japan (NAOJ) in order to demonstrate the technical feasibility of such slice mirrors (see Figure 7 right). We measured the surface roughness at dozens of different positions on the slit mirror by laser interferometer, WYKO NT1100, at the ATC of NAOJ. The obtained values of average roughness (Ra) were in the range of 10—25nm at any positions, showing that the sufficient mirror surface roughness for infrared observations was achieved for our test piece.
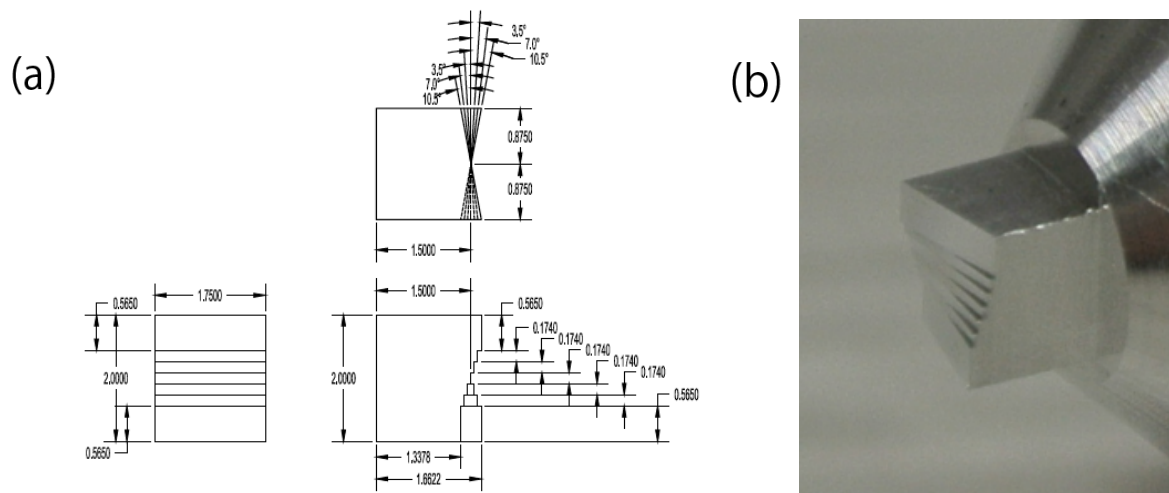
Figure 7. (a) The schematic design of the monolithic slice mirror for MRS-S. The scale is shown in units of mm. (b) The product image of the monolithic slice mirror for MRS-S made by the ultra-precision cutting machine, ULG-300, with single crystal diamond bits at the Advanced Technology Center (ATC) of NAOJ.

# ACKNOWLEDGEMENT

# REFERENCES

[1] Kataza, H., Wada,T., Sakon,I., Sarugaku, Y., Ikeda, Y., Fujishiro, N., Oyabu, S., "Mid-infrared camera and spectrometer on board SPICA", Proc. of SPIE, 8442, in this volume (2012)

[2] Matsuhara, H., Nakagawa, T., Kawakatsu,Y., Kawada, M., Murakami, H., Sugita, H., Shinozaki, K., Yamawaki, T., Sato, Y., Mitani, S., Crone, G., Issak, K.G., Heske, A., "Cooled scientific instrument assembly onboard SPICA", Proc. of SPIE, 8442, in this volume (2012)

[3] Nakagawa, T., Matsuhara, H., Kawakatsu, Y., "The next-generation infrared space telescope SPICA", Proc. of SPIE, 8442, in this volume (2012)

[4] Ootsubo,T., Onaka,T., Yamamura,I., Tanabe,T., Roellig,T.L., Chan,K.-W., Matsumoto,T., "IRTS Observations of the Mid-Infrared Spectrum of the Zodiacal Emission" , Advances in Space Research, 25, 2163-2166

[5] Reach, W. T., Morris, P., Boulanger, F., Okumura, K., "The mid-infrared spectrum of the zodiacal and exozodiacal light", Icarus, 164, 384-403 (2003)

[6] Roelfsema, P.R., et al. "The SAFARI imaging spectrometer for the SPICA Space Observatory", Proc. of SPIE, 8442, in this volume (2012)

[7] Swinyard, B. M., Rieke, G. H., Ressler, M., Glasse, A., Wright, G. S., Gerlet, M., Wells, M., "Sensitivity estimates for the mid-infrared instrument (MIRI) on the JWST", Proc. of SPIE, 5487, 785-793 (2004)

[8] Wada, T., Kataza, H., Matsuhara.H., Kawada,M., Ishihara, D., "Detector systems for the mid-infrared camera and spectrometer onboard SPICA", Proc. of SPIE, 8442, in this volume (2012)